ACS OMEGA

Open Access

http://pubs.acs.org/journal/acsodf

Article

Average Electron Density: A Quantitative Tool for Evaluating Non-Classical Bioisosteres of Amides

Alaa MA Osman and Alya A. Arabi*

Cite This: *ACS Omega* 2024, 9, 13172−13182

Read Online

ACCESS | Metrics & More | Article Recommendations | Supporting Information

ABSTRACT: Bioisosterism is strategically used in drug design to enhance the pharmacokinetic and pharmacodynamic properties of therapeutic molecules. The average electron density (AED) tool has been used in several studies to quantify similarities among nonclassical bioisosteres of carboxylic acid. In this study, the AED tool is used to quantify the similarities among nonclassical bioisosteres of an amide group. In particular, amide-to-1,2,3-triazole bioisosterism is considered. To evaluate the AED differences exhibited by isomers of nonclassical bioisosteres, both isomers of amide (*cis* and *trans*) and 1,2,3-triazole (1,4 and 1,5 disubstituted moiety) were considered. The amide and 1,2,3-triazole bioisosteric moieties were capped with various R groups (*R*= methyl, hydrogen, and chloro) to account for changes in their environment. Amide-to-triazole bioisosteric substitutions were then explored in a more realistic environment, that is, within the FDA-approved anticancer imatinib drug. The AED tool effectively identified similarities between substantially different moieties, 1,2,3-triazole and amide, showing AED differences of no more than 4%. The AED tool was also proven to be useful in evaluating the contribution of various factors affecting triazole-amide bioisosterism including isomerism and changes in their environment. The AED values of each bioisostere were transferable within a maximum difference of 2.6%, irrespective of the change in environment. The 1,4- and 1,5-disubstituted isomers of 1,2,3-triazole have AED values that differ by less than unity, 0.52%. Similarly, the AED values of the *cis*- and *trans*-amide isomers differ by only 1.31%. Overall, the AED quantitative tool not only replicated experimental observations regarding similarities in bioisosteres, but also explained and quantified each contributing factor. This demonstrates the extended utility of the AED tool from nonclassical carboxylic acid bioisosteres to amide equivalents.On the contrary, electrostatic potential maps, usually used in the literature to qualitatively evaluate bioisosterism, were not similar for the 1,2,3-triazole and amide bioisosteres, under different environments. Overall, the AED tool proves to be powerful in quantitatively evaluating and predicting bioisosterism across diverse moieties considering structural and environmental variations, making it valuable in drug design.

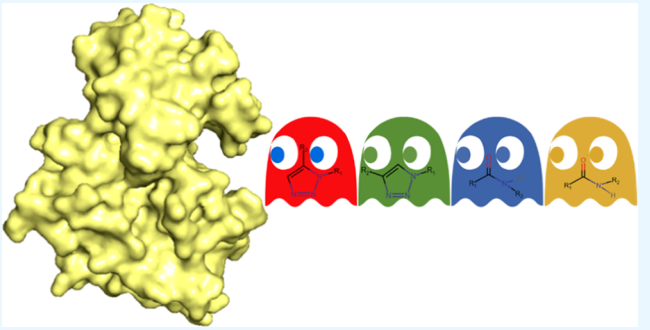

INTRODUCTION

Bioisosteres are groups which can be interchanged in a drug molecule while preserving its biological activity by maintaining similar interactions with its target receptor.[1,2] Bioisosteres that share a similar number of atoms, electrons,[3] peripheral layer of electrons,[4] shape, structure, electronic properties,[5] and/or physicochemical properties[6,7] are known as classical bioisosteres. For instance, the classical bioisosteres oxygen (−O−) and sulfur (−S−) share the same numbers of atoms and valence electrons, and benzene and pyridine share similar shapes with six-membered rings. The concept of bioisosterism was advanced to include not only classical bioisosteres but also nonclassical ones.[1] Nonclassical bioisosteres may not have the same electronic properties, structure, shape, number of atoms, or physicochemical properties.[1,2] However, they can still be interchanged in drug molecules without affecting their biological activity.[2] This is because many of them have been proven to have some common pharmacophore features and subsequently similar "key & lock" complementarity between a drug and its receptor.[8] For example, tetrazole ($-CHN_4$) and sulfonamide ($-SO_2NH_2$) are nonclassical bioisosteres of carboxylic acid (−COOH).[2,9]

The concept of bioisosterism is strategically useful in pharmaceutical and medicinal chemistry for designing new medications that preserve the bioactivities of existing drugs.[9] The ultimate target in bioisostere substitutions is to manipulate existing drug molecules to improve their pharmacokinetic and/or pharmacodynamic properties.[9] For example, replacing the carboxylic acid, in a molecule named EXP 7711,[10] with tetrazole generates a drug called Losartan. Losartan is an

Received: December 6, 2023
Revised: January 12, 2024
Accepted: February 7, 2024
Published: March 5, 2024

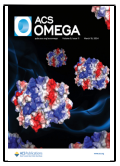

antihypertensive angiotensin II type I inhibitor that has better oral biological activity due to the lipophilicity of tetrazole.[9,11] Bioisosterism may also serve drug repurposing.[9] Another application of the nonclassical bioisosterism is in designing antibacterial "sulfa drugs" which function as competitive inhibitors of the enzyme dihydropteroate synthase.[9] "Sulfa drugs" have a common group, *p*-aminobenzoic acid, in which the carboxylic acid moiety is replaced with a sulfonamide bioisostere to improve the drug potency. Amide-to-1,2,3-triazole substitutions are also common[12] due to the structural features of triazole, *e.g.*, polarity, rigidity, as well as hydrogen bond donor and acceptor characteristics.[12] In particular, it is reported that the carbon atom (C_4, according to the IUPAC numbering style) in the 1,4-triazole moiety mimics the nitrogen atom (NH) in the amide group as a hydrogen-bond donor (see Figure 1). Whereas, the nitrogen atoms (N_2, N_3) in

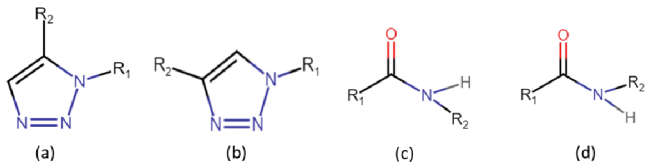

Figure 1. 2D structures of the bioisosteric moieties considered in this study: (a) 1,5-triazole, (b) 1,4-triazole, (c) *cis*-amide, and (d) *trans*-amide. The R_1 and R_2 denote different capping groups (benzene, methyl, and chloro).

the triazole ring mimic the amide bond since they serve as a weak hydrogen-bond acceptors (see Figure 1).[12−14] This bioisosteric replacement helps enhance binding affinities and improve chemical and metabolic stabilities of drug molecules.[15] Such substitutions have been tested in many drug molecules. For instance, they are employed in the HIV-1 inhibitors used to treat AIDS,[16] GPR88 agonists used as medications for neurological disorders,[17] 1-(*β*-D-glucopyranosyl)-4-substituted-1,2,3-triazoles used as antidiabetic medications that function by inhibiting glycogen phosphorylase b enzymes,[18] multiple/monotriazolominigastrins prescribed for cancer patients,[15] acetaminophen-triazole derivatives (APTDs) used as low hepatotoxic antipyretic medications,[19] triazole ceramide analogues used as inhibitors of cancer cell growth,[20] triazole-based tubulin inhibitors used as antitumor agents,[21] triazole-substituted Vismodegib used as anticancer drugs via inhibiting the Hedgehog (Hh) signaling pathway,[22] and triazole substituted imatinib (FA030) as ananticancer drug.[25,26]

Imatinib (Glivec, STI571) is an FDA-approved anticancer medication that functions by inhibiting the activity of Abl tyrosine kinase.[23] The activation of the Abl tyrosine kinase [by the breakpoint cluster region Abelson oncoprotein (BCR-Abl)] leads to uncontrollable cell growth, and therefore, the development of cancer, in particular, chronic myelogenous leukemia (CML).[24−26] Imatinib is one of the first cancer therapies, and it is a medication used worldwide to treat CML and various cancers.[25] However, one of the limitations that have been noticed in imatinib-treated cancer patients was developing drug resistance.[27] Therefore, the substitution of the amide in imatinib by a 1,2,3-triazole was tested to overcome the drug resistance complications and to possibly increase the potency of the drug.[27,28]

To evaluate the similarities among the amide and triazole nonclassical bioisosteres, two complementary tools were used. These are the average electron density (AED) tool[29−32] and the electrostatic potential (ESP) maps.[33,34] While the AED tool is a precise quantitative tool, ESP maps help visualize the key and lock complementarity between a drug molecule and its receptor. The ESP maps show the distribution of the negative and positive lobes in the molecules. They also help predicting the reactivities[35] as they show the electron-deficient and electron-rich parts of the molecule.[36] The concept of the AED tool is based on partitioning a molecule into atomic basins to compute the properties of selective groups, *e.g.*, bioisosteres, within a drug molecule. The partitioning scheme used in the AED tool is quantum theory of atoms in molecules (QTAIM). The average electron density of a bioisosteric group is given by $AED_{bioisostere} = \sum N_i/\sum V_i$, where $\sum N_i$ is the sum of the electron populations and $\sum V_i$ is the sum of the volumes of all atoms (each atom denoted by i) in the bioisosteric moiety.

In this study, the amide-triazole bioisosteric pair is selected for several reasons. These nonclassical bioisosteres are abundantly used in drug design.[28] However, the AED tool has not been tested, thus far, on moieties other than carboxylic acid and its bioisosteres, nor has it been evaluated for isomers of bioisosteres. This amide-triazole pair meets the criteria of diversity and bioisosterism. In addition, the selected bioisosteres have two isomeric forms each: the *cis* and *trans* constitutional isomers of amide, and the 1,4- and 1,5-positional isomers of triazole (see Figure 1). Furthermore, the amide and triazole moieties are surrounded by two capping groups. This is advantageous for investigating the effect of changes in environment beyond the alteration of a single capping group, as seen in previous studies.[29,30,32,37] To assess the validity of the AED tool on a more realistic system, the study is further extended to include bioisoteric substitutions in imatinib, an FDA-approved drug molecule, complexed with its Abl tyrosine kinase receptor.

METHODOLOGY

Capped Bioisosteres. A total of 36 molecules were considered. That is 2 bioisosteres (amide and triazole) × 2 isomers each (*cis*-amide, *trans*-amide, 1,4-triazole, and 1,5-triazole as shown in Figure 1) × 9 different combinations of R_1 and R_2 each. The 9 different combinations of R_1R_2 are BB, BCl, BM, ClB, ClCl, ClM, MB, MCl, and MM, where B, Cl, and M stand for benzene, chloro, and methyl, respectively. The groups were chosen according to their abundance in drug molecules[38] and their wide range of electronegativities. The 36 molecules were optimized in the gas phase using the Gaussian 16 package.[39] The hybrid B3LYP density functional method was used with a triple-*ζ* Pople basis set, 6-311++G(d,p), and ultrafine pruned (99,590) grids. The self-consistent field optimization criteria were set to "tight." No symmetry was used during the optimization. Frequency calculations were completed to confirm that the optimized geometries are not transition states. To evaluate the AED values of the bioisosteric moieties, the atomic integrations were performed using the AIMAll package (14.11.23),[40] which is based on the QTAIM partitioning scheme.[41,42] The Lagrangian values were small; they did not exceed milli atomic units (au). Three different isodensity envelopes (0.0004, 0.001, and 0.002 au) were considered. The ESP maps of the capped bioisosteres were generated using ChemCraft 1.8 (https://www.chemcraftprog.com).

Imatinib and its Analogues. This study also considers bioisosteric replacements in the FDA-approved drug, imatinib.

https://doi.org/10.1021/acsomega.3c09732
ACS Omega 2024, 9, 13172−13182

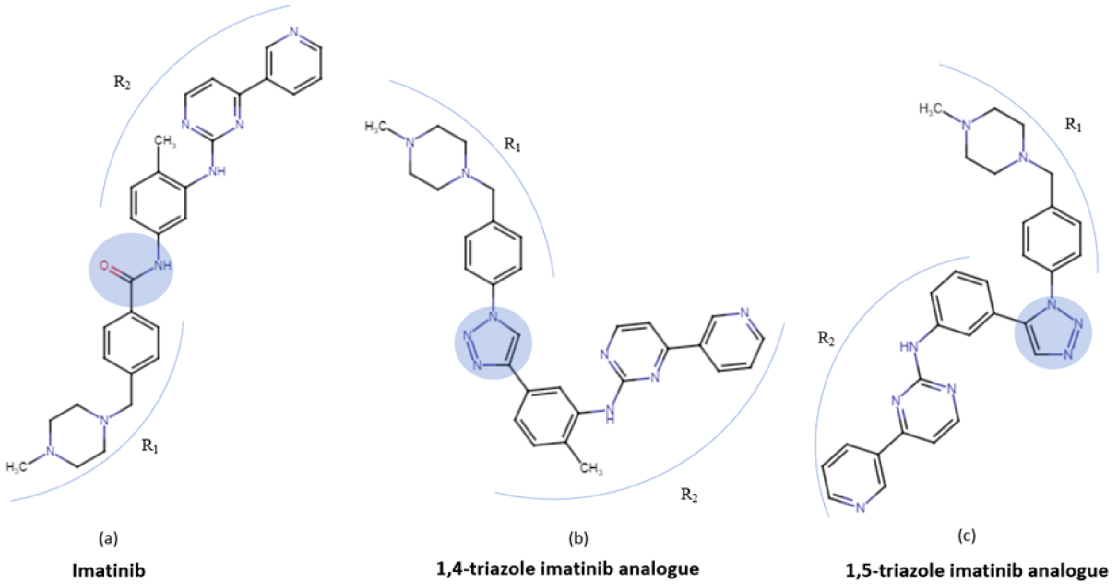

Figure 2. 2D structures of (a) the imatinib drug, (b) its 1,4-triazole-analogue, and (c) its 1,5-triazole-analogue. The amide bioisosteric group in imatinib and the triazole group in its analogues are highlighted in blue, and the capping groups are denoted by R_1 and R_2.

This drug comprises an amide bioisostere capped with two R groups (depicted in Figure 2), which are termed as realistic R groups.

In this study, the amide group in imatinib is replaced with 1,4- and 1,5-triazole, forming two analogue structures. The imatinib and its analogues were prepared, and the amide-to-triazole bioisosterism was evaluated using the following steps:

1) The imatinib drug molecule was extracted from an imatinib-Abl tyrosine kinase complex obtained from the RCSB database (https://www.rcsb.org/structure/2hyy) (PDB ID: 2HYY).[26] Triazole analogues of imatinib were built by replacing the amide group with 1,4- and 1,5-disubstituted 1,2,3-triazoles (Figure 2).
2) Conformers of imatinib and its triazole analogues were generated using OpenEye's Omega 4.2. 0.1 tool.[43]
3) Using the Fred tool in OpenEye,[44,45] the generated conformers of imatinib and its analogues were docked into the Abl tyrosine kinase receptor.[26−28] The entire receptor was considered for docking (the box size is 39.67 Å × 65.00 Å × 52.67 Å with a volume of 135 792 $Å^3$). The docking scores of the top-ranked conformers of each of the imatinib and its analogues were reported. The docking scores are based on the unitless Chemgauss4 scoring function.
4) The Gaussian 16 package[39] was used to run single point calculations, at the B3LYP/6−311++G(d,p) level with ultrafine pruned (99,590) grids, on the top-ranked conformers of imatinib and its analogues. The electronic energies were collected and used as an estimate of the stability of the molecules.
5) AIMALL analysis was then performed using the AIMAll package (14.11.23)[40] (as described above) to obtain the AED of the amide and triazole bioisosteric moieties in imatinib and its analogues.
6) The ESP maps of the docked complexes were generated using the VIDA 4.4.0.4 molecular visualization too, OpenEye Scientific Software.[46] ESP maps of the docked structures shall help confirm the similarities in some pharmacophore features of the replaced bioisosteric groups.[47]

RESULTS AND DISCUSSION

Capped Bioisosteres. Thirty-six molecules were considered in this part of the study. These molecules were constructed by using 2 bioisosteres × 2 isomers per bioisostere × 3 R_1 capping groups per isomer × 3 R_2 capping groups per isomer. Each of the R_1 and R_2 capping groups can be a benzene, a chloro, or a methyl group. In the forthcoming sections, the AED results are discussed, followed by the ESP results for the capped bioisosteric moieties: 1,4-triazole, 1,5-triazole, *cis*-amide, and *trans*-amide.

AEDs of the Capped Bioisosteres. The AED values of all molecules were evaluated at three different isodensity values (0.002, 0.001, and 0.0004 au). It is noted that the AED values have the same trends across the three isodensities, even though the absolute values are different (see Figure S1). Therefore, for the rest of this study, unless otherwise specified, all AEDs will be reported at a single isodensity value, namely 0.001 au. The volumes, electron populations, charges, AEDs, electronic energies, and distances related to the 36 molecules studied in this section are summarized in Table 1. Prior to discussing the AEDs, it is noted from the average electronic energies reported in this table that the capped triazoles are more stable than the capped amides. This is aligned with the experimental fact that the triazole-containing medications (such as Leu-enkephalin/Leu-Enk) exhibit an extended biological half-life.[48,49] The *trans*-amide is, on average, more stable than the *cis*-amide by 2.7 kcal/mol, which matches with the ∼2.6 kcal/mol value reported in the literature.[50]

At an isodensity of 0.001 au, the average AED values (over different R groups) of 1,4-triazole, 1,5-triazole, *trans*-amide, and *cis*-amide are 0.0726, 0.0722, 0.0744, and 0.0734 au, respectively (Table 1). This remarkable similarity in the AED values of the four bioisosteric moieties confirms the validity of the AED tool in capturing similarities among bioisosteres, no matter how diverse they are. The small standard deviations in AEDs reflect the similarity in the AEDs of a given bioisostere,

https://doi.org/10.1021/acsomega.3c09732
ACS Omega 2024, 9, 13172−13182

Table 1. This Table Summarizes the Key Properties (Averaged per Bioisostere, Across Different R Groups ± Standard Deviations) of the 36 Molecules Studied in this Section[a]

	properties (on average) of the bioisosteric moieties				average AEDs of the R capping groups		average molecular properties of the whole molecule (bioisosteric moiety + R capping group)		
entity	volume (au)	electronic population (au)	charge (au)	AED (au)	R_1 AED (au)	R_2 AED (au)	electronic energies (au)	atomic intramolecular distances (Å)	atomic intramolecular distances (Å) references[b]
1,4-triazole	472.43 ± 5.19	34.28 ± 0.19	−0.40 ± 0.19	0.0726 ± 0.0007	0.059 ± 0.018	0.058 ± 0.017	−728.9806 ± 258	4.8 ± 0.71	5.0−5.1
1,5-triazole	475.19 ± 3.80	34.30 ± 0.18	−0.43 ± 0.18	0.0722 ± 0.0004	0.059 ± 0.018	0.059 ± 0.017	−728.9779 ± 258	3.0 ± 0.62	2.4−3.1
cis-amide	299.03 ± 4.83	22.24 ± 0.20	−0.31 ± 0.19	0.0734 ± 0.0006	0.058 ± 0.016	0.059 ± 0.017	−656.6417 ± 258	3.1 ± 0.1	2.4−2.9
trans-amide	302.80 ± 3.95	22.23 ± 0.19	−0.32 ± 0.20	0.0744 ± 0.0011	0.058 ± 0.016	0.059 ± 0.017	−656.6460 ± 258	4.0 ± 0.14	3.8−3.9
triazole (average of 1,4 and 1,5 isomers)	473.81 ± 4.63	34.29 ± 0.18	−0.41 ± 0.18	0.0724 ± 0.0006	0.059 ± 0.017	0.058 ± 0.016	−728.9793 ± 250	NA	NA
amide (average of *cis* and *trans* isomers)	300.92 ± 4.70	22.24 ± 0.19	−0.32 ± 0.19	0.0739 ± 0.0010	0.058 ± 0.016	0.059 ± 0.017	−656.6439 ± 250	NA	NA

[a]To the left are the average volumes (au), electronic populations (au), charges (au), and AEDs (au) of the triazole and amide bioisosteric moieties in the molecules. In the middle are the AEDs of the capping R groups in the molecules. To the right are the average electronic energies (au) of the molecules and key intramolecular distances (Å). All values are reported at an isodensity of 0.001 au. NA stands for "not applicable". [b]References 13, 28, 51, and 52 ; the listed range covers the values reported in all the cited studies.

irrespective of its environment. This confirms the power of transferability that this tool can offer. It is observed that the AED values of the bioisosteric moieties gradually decrease with the change of the R_2 groups in the following order: benzene, chloro, methyl (see Figure S1). It is noted that the AEDs of the *trans*-amide capped with a benzene R_2 group are exceptionally slightly greater than the AEDs of the same moiety capped with a chloro or a methyl group.

At an isodensity of 0.001 au, the highest (0.0763 au) and the lowest (0.0714 au) AED values across all 36 molecules are off by only 6.3%. This is a very small deviation provided all the differences in the cyclic vs noncyclic shapes of the bioisosteres, the *cis*/*trans* constitutional isomerism in the amide moiety, the 1,4/1,5 positional isomerism in the triazole moiety, and the combination of 9 different environments per isomer. Therefore, the AED tool robustly captures the similarity between the amide and triazole nonclassical bioisosteres, irrespective of the isomerism and/or the changes in the environment. As reported in previous studies,[29−32,37] this similarity is not by serendipity provided that the capping R groups can have AEDs that differ by up to 300%.[37] Similarly, the R groups in this study have sporadic AEDs that differ by up to 97% (Figure S2). In addition, as a counter example, this similarity is not applicable for the furan and the sulfonamide moieties, which are not used in the literature as bioisosteres of each other, despite each of them being separately a bioisostere of carboxylic acid.[37] These two non-bioisosteric moiteis have AED values that are off by up to 34%.

Irrespective of isomerism, the similarity in the AED of the amide and triazole bioisosteres is remarkable despite the significant differences in their respective electron populations and volumes, and despite the high fluctuations in their respective charges (as obvious from the large standard deviations reported in Table 1) (see also Figure S3). For instance, on average, the atomic volumes of 1,4-triazole/1,5-triazole and *trans*-amide/*cis*-amide are 472/475 and 299/302 au, respectively; while the corresponding electron populations are 34.3/34.3 and 22.2/22.2, respectively. It is noted that the average atomic volumes of triazole are off by ∼58% compared with those of amide, and similarly, their electron populations are off by ∼54%. The electronic population-to-volume ratios (*i.e.*, AEDs) are remarkably similar, with a maximum difference of 2.96% (see Figure 3). It is worth noting that the volumes of the isomers of a given bioisostere exhibited only slight differences, whereas their corresponding electron populations are identical (Table 1). Hence, the difference in the electronic volumes is the main factor that resulted in 0.52% or 1.31% in the AEDs of the 1,4/1,5 or *cis*/*trans* isomers, respectively (Figure 3). These small percent differences among isomers of a given bioisostere correspond to only 0.001 au, which is an order of magnitude smaller than the maximum difference between the amide and triazole groups (0.022 au).

Figure 3 is a schematic diagram that summarizes the AED differences as a result of all possible combinations of isomeric bioisosteric substitutions as well as changes in the environment based on the 36 molecules covered in this section.

In Figure 3, the percent AED difference attributed to bioisosterism is defined as the difference between the new and existing bioisosteres relative to the original moiety, *i.e.*, amide. The %AED differences are evaluated as follows:

$$\frac{\mathrm{AED}_{cis\text{-amide}} - \mathrm{AED}_{1,4\text{-triazole}}}{\mathrm{AED}_{cis\text{-amide}}} \times 100 = 1.16\% \quad (1)$$

https://doi.org/10.1021/acsomega.3c09732
ACS Omega 2024, 9, 13172−13182

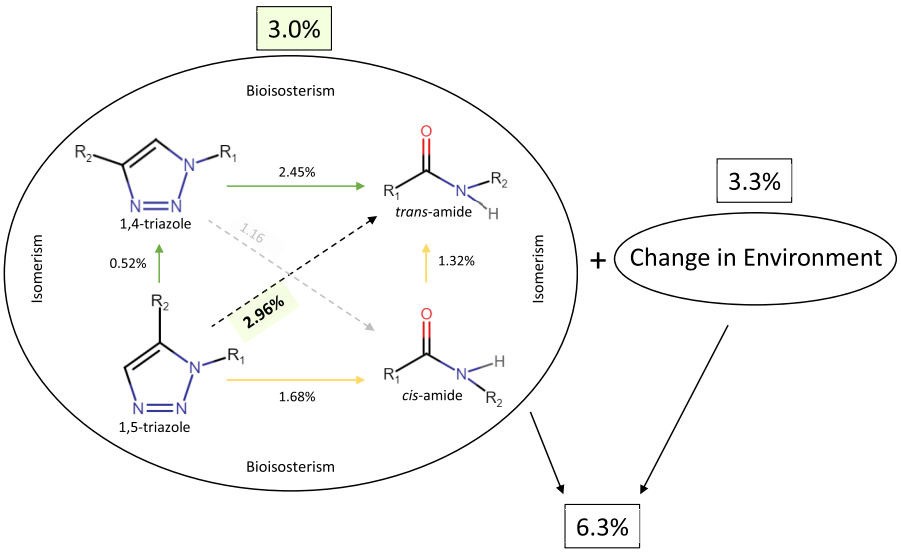

Figure 3. AED differences among bioisosteres. The maximum percent difference is 6.3%, 3.0% of which is attributed to the change in bioisosteres including the isomerism effect, and the remaining 3.3% is attributed to the change in environment (*i.e.*, change in R groups, and possibly the 3D orientation of the R groups).

$$\frac{\mathrm{AED}_{cis\text{-amide}} - \mathrm{AED}_{1,4\text{-triazole}}}{\mathrm{AED}_{cis\text{-amide}}} \times 100 = 1.68\% \quad (2)$$

$$\frac{\mathrm{AED}_{trans\text{-amide}} - \mathrm{AED}_{1,4\text{-triazole}}}{\mathrm{AED}_{trans\text{-amide}}} \times 100 = 2.45\% \quad (3)$$

$$\frac{\mathrm{AED}_{trans\text{-amide}} - \mathrm{AED}_{1,5\text{-triazole}}}{\mathrm{AED}_{trans\text{-amide}}} \times 100 = 2.96\% \quad (4)$$

$$\frac{\mathrm{AED}_{\mathrm{amide}} - \mathrm{AED}_{\mathrm{triazole}}}{\mathrm{AED}_{\mathrm{amide}}} \times 100 = 2.07\% \quad (5)$$

In eqs 1−5, the AED value for each bioisosteric moiety represents the average AED across all nine molecules, each having the moiety capped with nine different combinations of R_1 and R_2 groups.

Figure 3 depicts the remarkable similarities in the AEDs of the bioisosteres. The maximum difference, which corresponds to 0.022 au (*i.e.*, 2.96%), is between those of 1,5-triazole and *trans*-amide. The total of 6.3% reported in this figure is the percent difference between the lowest AED (0.7150 au for the 1,4-triazole moiety capped with two methyl groups) and the highest AED (0.0763 au for the *trans*-amide capped with two benzene groups) of the bioisosteric moieties across all 36 molecules. Therefore, out of the total AED difference of 6.3%, 3.0% is attributed to bioisosterism including isomerism, and the remaining 3.3% is attributed to the change in environment. It is worth noting that, considering direct evaluations of the change in environment, the percent differences between the lowest and highest AED values of a given bioisosteric moiety capped with nine different combinations of R_1 and R_2 groups are 3.1%, 1.7%, 4.5%, and 2.6% for 1,4-triazole, 1,5-triazole, *trans*-amide, and *cis*-amide, respectively, with an average of 3.0% across the four bioisosteric moieties.

On average, the AED of all the amides (0.0739 au) is slightly greater, by 2.07%, than that of all the triazoles (0.0724 au). This difference in the AEDs of amide and triazole is within the range of differences reported in the literature for carboxylic acid and its bioisosteres, *e.g.* tetrazole (0.2%),[25] sulfonamide (26.2%),[26] or isoxazole, tetrazole-5-one, oxadiazole, thiazolidinedione, and oxazolidinedione (4.6%).[29,30,32] Considering isomerism, the AED of the *trans*-amide is 1.31% greater than that of the *cis*-amide, irrespective of the R groups. Similarly, the AED of 1,4-triazole is 0.52% greater than that of the 1,5-triazole isomer, irrespective of the R groups.

As documented in previous experimental studies, 1,4-triazole is a common bioisosteres of *trans*-amide, while 1,5-triazole is a common replacement of *cis*-amide.[12,13,16,28,48,51,52] As shown in Table 1, the intramolecular distance between the first atoms of the two R groups in *trans*-amide (3.8−3.9) is reported to be ∼75% similar to those of 1,4-triazole (5.0−5.1 Å). Likewise, these distances in *cis*-amide (2.4−2.9) and 1,5-triazole (2.4−3.1) are up to 100% similar. Table 1 also shows the close similarities between the experimentally reported distances and the measured distances from the computationally optimized geometries in this study: 4.8 ± 0.71, 3.0 ± 0.62, 3.1 ± 0.1, and 4.0 ± 0.14 for 1,4-triazole, 1,5-triazole, cis-amide, and trans-amide, respectively. In addition, our AED results reproduced the experimental observation of 1,4-triazole being a better replacement than 1,5-triazole for the amide moiety, although the preference is not a major one. The AED difference between 1,4-triazole and *trans*-amide is 2.45%, while this difference is 2.96% between 1,5-triazole and *trans*-amide (Figure 3). However, unlike the literature records, our data suggest that there is a preference of 1,4-triazole over 1,5-triazole for the *cis*-amide, although a minute preference by only 0.52% (*i.e.*, the difference between 1.68% and 1.16% from eqs 1 and 2). However, this difference is too small to be overinterpreted.

Using the Swissbioisostere database (http://www.swissbioisostere.ch/, as of August 2022), the 1,4-triazole-to-amide search results in 83 hits, which is significantly greater than the 7 hits obtained for the 1,5-triazole-to-amide search (note that the Swissbioisostere Web site accepts the amide only in its *trans* form). In addition, the Swissbioisostere database reports the difference in bioactivity (Δactivity) as a measure to evaluate the extent of bioisosterism between the chosen moieties, referred to as molecular matched pair (MMP). If Δactivity, *i.e.*, specifically the half maximal inhibitory concentration (IC_{50}) in this case, is greater than 0.5 log

https://doi.org/10.1021/acsomega.3c09732
ACS Omega 2024, 9, 13172−13182

units, then the pair has a better match. If the Δactivity is smaller than −0.5 log units, then the moieties are likely not good bioisosteres of each other.[53] Based on the ΔIC_{50} measures, the highest Δactivity between amide and 1,5-triazole is 0.54 log units, while this difference reaches 1.44 log units with 1,4-triazole. This suggests that 1,4-triazole and amide are better molecular matched pairs than 1,5-triazole and amide. The conclusions from (i) experimental observations, (ii) experimental and computational distances, (iii) our calculated AEDs, and (iv) the number of hits as well as the Δactivity records in Swissbioisostere are all in perfect agreement favoring the 1,4-triazole (over 1,5-triazole) as a bioisosteric replacement of *trans*-amide.

ESP Maps of the Capped Bioisosteres. The electrostatic potential maps of the four bioisosteric moieties considered in this study, each capped with 9 different combinations of R_1 and R_2 groups, are depicted in Figure 4.

It is obvious from Figure 4 that the four bioisosteric moieties share similarities in their ESP maps. They all have two separate negative lobes (or a single merged lobe) (in purple) surrounding the oxygen atom in the amide group and two negative lobes surrounding the nitrogen atoms (N_2, N_3) in the triazole ring. These noticeable similarities in the ESP maps of the bioisosteric moieties, despite the differences in their identity and/or their capping R groups, illustrate visually the potential of these bioisosteres to interact similarly with a given receptor and, therefore, to exhibit similar biological activities. There are cases where the negative lobes (in purple) are too large and close to each other that they merge into one bigger lobe include the *cis*-amide with R_1=chloro, and *trans*-amide with R_1=chloro or R_2=benzene. This difference in the number of the negative lobes (one vs two) may potentially mislead the visual comparisons and, thus, the evaluations of the "key & lock" similarities between the drug molecule and its receptor. This ambiguity in the ESP maps is contrasted with the precise detection of bioisosteres through the AED tool, where the maximum difference among all 36 molecules is 6.3%.

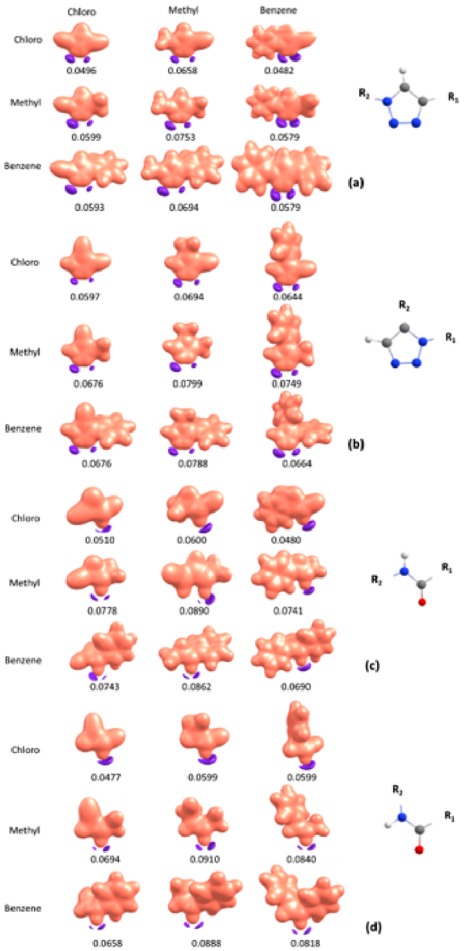

Figure 4. Electrostatic potential maps of (a) 1,4-triazole (rows 1−3), (b) 1,5-triazole (rows 4−6), (c) trans-amide (rows 7−9), and (d) cis-amide (rows 10−12). The 2D structures of the four bioisosteric moieties are included to show the corresponding positions of R_1 and R_2 in the maps. Each of the four bioisosteric moieties is capped with 9 different combinations of R_1 (labeled to the left) and R_2 groups (labeled at the top). The molecular isodensity values are reported (in au, *i.e.*, e^-/a_0^3) for each molecule. The purple color indicates negative, and the salmon color indicates positive values of electrostatic potentials.

Imatinib and its Analogues. In this section, the amide-to-1,4-triazole and amide-to-1,5-triazole replacements in imatinib are considered. Imatinib and its analogues are docked into their receptor, Abl tyrosine kinase enzyme. The docking results are discussed first, followed by those of the ESP maps. The AED values are discussed at the end of this section.

Molecular Docking of Imatinib and its Analogues. Each of the 1,4- and 1,5- analogues was docked into Abl tyrosine kinase. To compare the poses and the binding site of the docked imatinib and its analogues, the docked structures, along with the experimental complex (PDB: 2HYY), are shown in Figure 5.

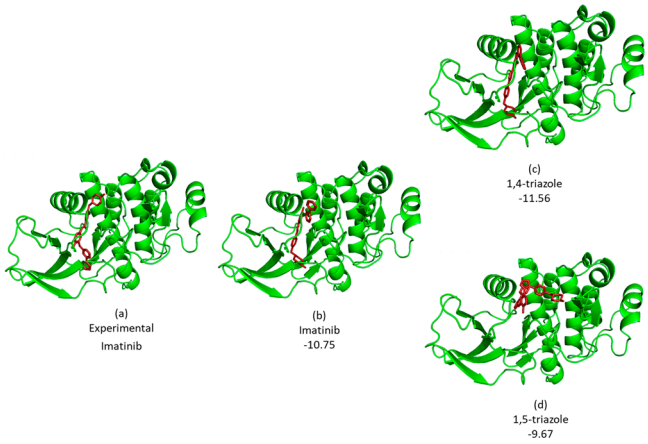

Figure 5. (a) Crystal structure of imatinib complexed with Abl tyrosine kinase (PDB ID: 2HYY). The rest of the complexes are docked structures of different ligands in the same receptor: (b) imatinib, (c) the 1,4-triazole-analogue of imatinib, and (d) the 1,5-triazole-analogue of imatinib. The Fred Chemgauss4 docking scores are reported under each docked complex.

As depicted in this figure, the imatinib and its 1,4-triazole analogue share the same binding pocket in their target, while the 1,5-triazole prefers binding in a slightly different pocket, although in the same vicinity of the experientially determined active site. This could be due to, among other reasons, the steric effect of 1,5-triazole.[28] This also indicates that in a realistic environment (*i.e.*, a bioisosteric moiety in an FDA-approved drug molecule docked in its receptor), the amide is better replaced with 1,4-triazole than 1,5-triazole. This

https://doi.org/10.1021/acsomega.3c09732
ACS Omega 2024, 9, 13172−13182

Table 2. Interacting Residues in the Binding Pocket of the Abl Tyrosine Kinase Receptor[a]

imatinib experimental, ref 26	1,4-triazole analogue computational, ref 27	imatinib computational, this study	1,4-triazole analogue computational, this study	1,5-tirazole analogue computational, this study
	Leu248	Leu248	Leu248	
	Tyr253	Tyr253	Tyr253	
	Val256	Val256	Val256	
		Ala269	Ala269	
	Lys271		Lys271	Lys271
Glu286		Glu282		
		Glu286	Glu286	Glu286
	Val289	Val289	Val289	Val289
		Met290	Met290	Met290
		Ile293	Ile293	Ile293
			Leu298	
		Val299	Val299	
	Ile313			
Thr315	Thr315	Thr315	Thr315	
		Glu316		
	Phe317		Phe317	
Met318	Met318			
	Gly321		Gly321	
			Leu354	Leu354
				Phe359
Ile360	Ile360			Ile360
His361	His361			
				Arg362
	Leu370	Leu370	Leu370	
Ala380	Ala380	Ala380	Ala380	
	Asp381	Asp381	Asp381	Asp381
	Phe382	Phe382	Phe382	Phe382
		Gly383	Gly383	Gly383
				Ser385
Tyr393				
				Ala399
				Lys400
				Phe401

[a]Both experimental and computational data from previous studies are reported. Common residues are aligned across different columns.

observation aligns with the findings discussed in the Capped Bioisosteres section.

The molecular docking scores for imatinib and its 1,4-triazole and 1,5-tirazole analogues are −10.75, −11.56, and −9.67 Fred Chemgauss4 score, respectively. The difference in the docking scores of imatinib and its 1,4-triazole analogue is approximately unity. This is consistent with the unity difference which is also observed in the previously reported docking scores (*i.e.*, −13.7 and −12.7 for imatinib and the 1,4-triazole-containing analogue, FA030).[27]

Replacing the amide moiety in imatinib with the 1,4-triazole bioisostere slightly enhances the docking Fred Chemgauss4 score from −10.75 to −11.56. This improvement in the binding score is accompanied by a greater number of reported binding site residues, particularly through hydrogen bonding (three hydrogen bond donor/acceptor sites vs only two of them in imatinib). This analogue is reported to have a higher dipole moment of ∼4.5 D, while that of amide is ∼3.5 D.[28] These findings align with the results obtained from in vitro and in vivo experiments conducted to validate the effectiveness of the 1,4-triazole analogue in enhancing the properties of imatinib as an antineoplastic medication. These experiments aimed to validate the anticancer effect of the new 1,4-triazole analogue, while reducing the patients' resistance to imatinib.[27,28] These studies reported similar enzymatic activity of the 1,4-triazole analogue (FA030) and imatinib as they share similar IC_{50} values (10.97 ± 0.46 and 10.77 ± 0.41, respectively). In addition, FA030 was shown to have antiapoptotic effects and a significant antiproliferative activity in cancer cell lines.[27]

Table 2 lists the amino acid residues within the Abl tyrosine kinase receptor that have been reported in the literature to bind with imatinib or its analogues. These include results from *i)* an experimental study by Cowan-Jacob *et al.* (using X-ray crystallography),[27] *ii)* a computational study by Arioli *et al.* (using the Extra Precision Glide docking software),[27] and *iii)* this study (using the OpenEye software). For the 1,4-triazole analogue, there is a high overlap of 12 residues commonly reported by ref 27 and this study. This is indicative that the data of the two different docking methods are, to a large extent, reproduced.

The findings of this study reveal that the computationally complexed imatinib, 1,4-triazole analogue, and 1,5-triazole analogue have three common binding residues (Glu282, Thr315, Ala380), two common binding residues (Thr315, Ala380), and one common binding residue (Ile360), respectively, with the experimentally complexed imatinib (see Table 2). In addition, considering the results of this study, the

https://doi.org/10.1021/acsomega.3c09732
ACS Omega 2024, 9, 13172−13182

1,4-triazole analogue shares 15 residues with imatinib, while the 1,5-triazole analogue shares only 7 residues with imatinib. These observations complement the ones made in Figure 5 and are in full alignment with the experimentally observed preference of 1,4-triazole over 1,5-triazole as a bioisostere of imatinib. The differences in some of the reported residues (compared to residues reported in previous studies) could be attributed to *i)* variations in the experimental/computational protocols used, *ii)* differences in the defined thresholds used to determine the presence or absence of interactions, and *iii)* slight variations in poses that facilitate contact with distinct residues. This molecular docking also demonstrates that the conclusions drawn from the isolated capped moieties are reproducible with those obtained from the embedded drug molecule within its receptor.

ESP Maps of the Complexed Imatinib and its Analogues in their Receptor. The ESP maps are used as a complementary visual tool to evaluate the amide-to-triazole bioisosterism. Figure 6 illustrates the electrostatic potential maps of the top-ranked conformers of imatinib and its two triazole analogues complexed with Abl tyrosine kinase.

The ESP maps across the three complexes have distinct features. This is not unexpected provided that the ESP maps are influenced by ligand−target interactions,[28−30,46] and that (as shown in Figure 5 and Table 2) the interactions vary among these three complexes. However, these three complexes do share general similarities among their ESP maps. They all have a big negative (red) lobe around the center of the molecule (specifically around the oxygen atom of the amide bioisostere, or around the nitrogen atoms of the triazole bioisostere), and two smaller negative lobes on either side of the big negative lobe. However, between the 1,4-triazole and the 1,5-triazole analogues, the former demonstrates a better resemblance to imatinib. The AED tool successfully reproduced this observation quantitatively. This emphasizes the capacity of the AED tool to implicitly account for the "key & lock" complementarity between the drug molecule and its receptor. This is a very distinguished and powerful attribute of the AED tool.

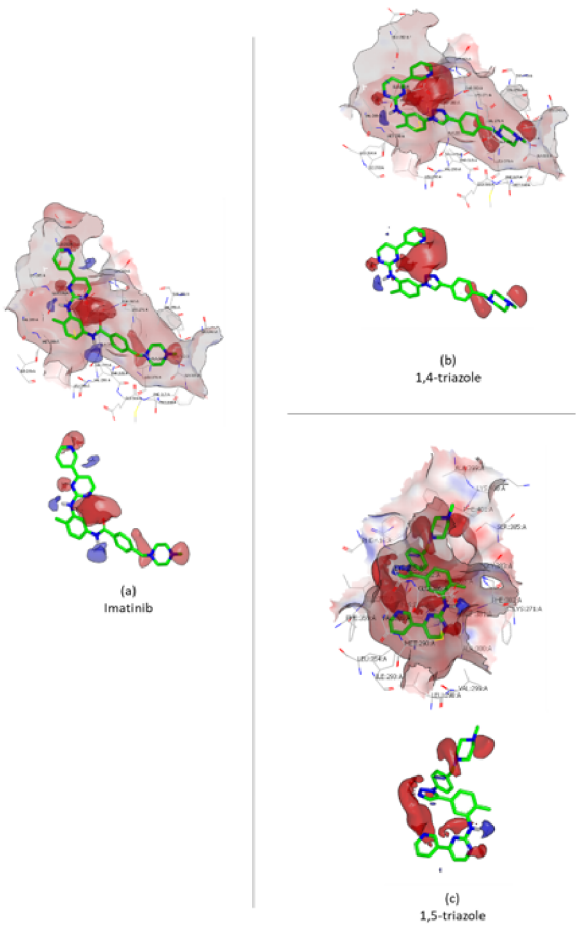

Figure 6. Electrostatic potential maps, at an isodensity of 0.985 au, of the docked (a) imatinib, (b) 1,4-triazole-analogue, and (c) 1,5-triazole-analogue in the Abl tyrosine kinase receptor. The ESP maps are shown for the ligand-receptor complex and for the ligand alone for facilitating comparisons.

AEDs of Imatinib and its Analogues. In this section, we will demonstrate the power of the AED tool in evaluating the nonclassical amide-to-triazole bioisosterism in an FDA approved drug molecule, imatinib. We also highlight the reproducibility and transferability of the AED values.

Figure 7 is a schematic summary of all of the AED differences resulting from the amide-to-triazole bioisosteric replacement in imatinib. It also includes the capped bioisosteric moieties from the previous section for facilitating comparisons.

Compared to imatinib, the 1,4- and 1,5-triazole analogues exhibit reduced AEDs by approximately 2% and 4%, respectively (Figure 7). Thus, compared to the AED of the amide in imatinib the 1,4-triazole has a closer value than the 1,5-triazole. Therefore, not only does the 1,4-triazole outperform the 1,5-triazole in terms of docking scores and binding poses (as discussed above), but it also outperforms it in terms of AED similarities with respect to the original amide bioisostere. These cumulative observations indicate that the 1,4-triazole substitution is a more favorable bioisosteric replacement for the amide than the 1,5-triazole. Furthermore, the AED analysis effectively detects the subtle differences within a *ca.* 2% range among the 1,4-triazole and 1,5-triazole analogues. The difference in the AED values does not exceed 3% or 4% as a result of the bioisosteric substitutions in the capped molecules or imatinib, respectively. This confirms the similarity in the AED values of the bioisosteric moieties, irrespective of their environment. In fact, the first section in this study confirms this concept of transferability in AEDs, regardless of the chosen R_1 or R_2 groups. In addition, based on this study, changes in environment account for the following percent deviations in the AED values of the bioisosteric moieties: 1.42%, 2.62%, or maximum 3.34% (see Figure 7). Similarly, this value is *ca.* 5% based on previous studies.[46]

Overall, it is concluded from this section that the AED differences due to the amide-to-triazole bioisosterism in imatinib are very low, typically below 4%. In addition, the AED tool meticulously detects the effect of various factors (change in environment, isomerism, and bioisosterism) in an additive manner (see Figure 7). In other words, the AED tool interestingly captures the individual and combinatorial influence of different factors in nonclassical bioisosterism. These findings demonstrate that the AED tool consistently provides reproducible, precise, robust, and transferable evaluations in nonclassical bioisosterism.

https://doi.org/10.1021/acsomega.3c09732
ACS Omega 2024, 9, 13172−13182

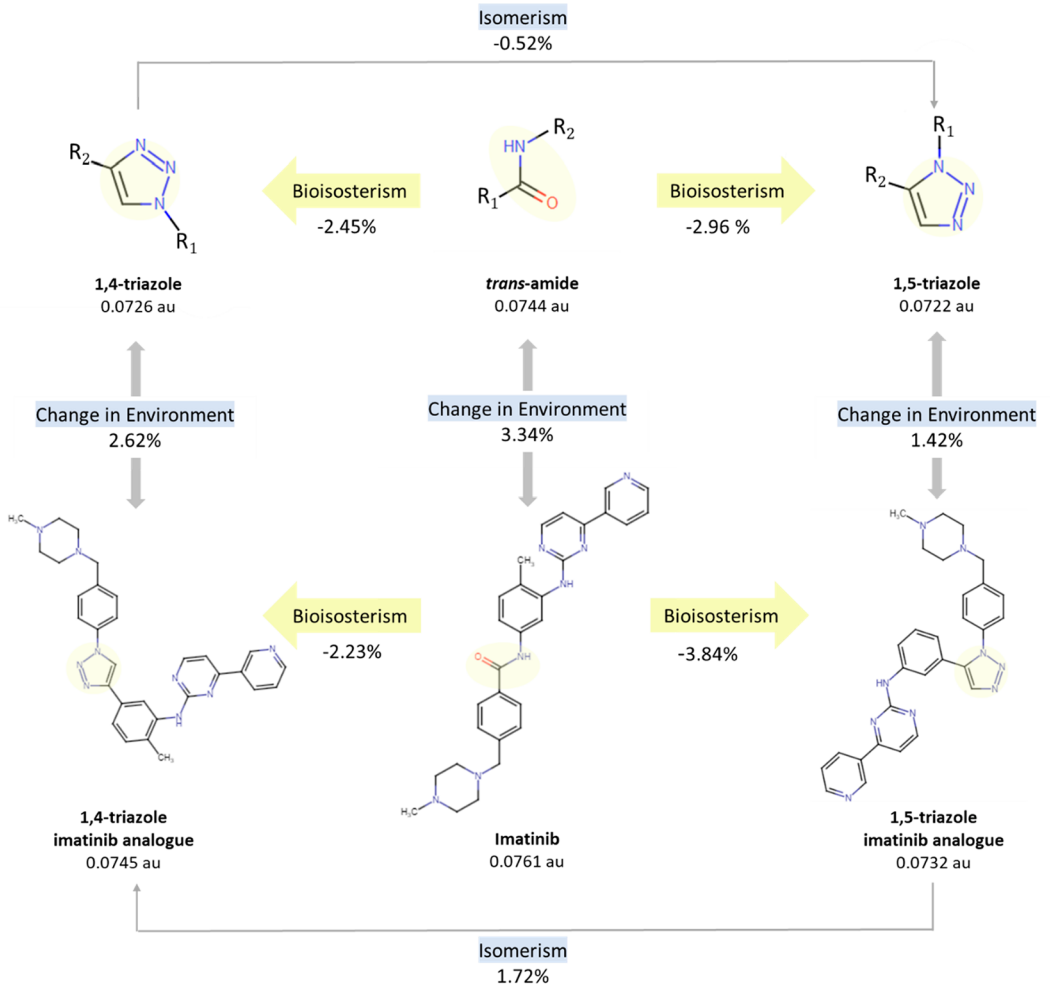

Figure 7. A summary of the AED differences among amide and 1,2,3-triazole bioisosteres in their different isomers, and in different environments. The value reported under each structure is the average AED (in au) of the bioisosteric moiety (highlighted in yellow) in this structure.

CONCLUSIONS

In conclusion, the validity and robustness of the AED tool in quantitatively evaluating similarities among bioisosteres have been proven to extend to the amide-to-triazole bioisosterism, with a high percent AED similarity exceeding 96%. The tool was shown to be precise enough to meticulously differentiate isomers (*cis*/*trans* constitutional iomers ofamide and 1,4/1,5 positional isomers of triazole). This tool also accurately replicated the experimentally observed trend of 1,4-triazole being a more suitable substitute than 1,5-triazole for the *trans*-amide. The transferability and reproducibility of the AED tool have been confirmed by comparing the results of the capped bioisosteres with those of the moieties embedded in a realistic environment, compromising an FDA-approved drug molecule docked within its receptor. The differences in the AED values did not exceed 4% as a result of changing the environment of the bioisostere. While depending solely on ESP maps is not entirely reliable, they can serve as a valuable qualitative complement to the robust AED tool for evaluating bioisosterism.

ASSOCIATED CONTENT

Supporting Information

The Supporting Information is available free of charge at https://pubs.acs.org/doi/10.1021/acsomega.3c09732.

Figure S1 and Figure S2 depict the average electron densities of the bioisosteric moieties and the R groups, respectively, for the 36 molecules discussed in the Capped Bioisosteres section. Figure S3 shows the average volumes, average electron populations, and charges of the bioisosteric moieties in the same section (Capped Bioisosteres). The coordinates of the molecules can be provided upon request (PDF)

AUTHOR INFORMATION

Corresponding Author

Alya A. Arabi − *College of Medicine and Health Sciences, Department of Biochemistry and Molecular Biology, United Arab Emirates University, AlAin 15551, United Arab Emirates;* orcid.org/0000-0003-3664-314X; Email: alya.arabi@uaeu.ac.ae, alya.arabi@dal.ca

Author

Alaa MA Osman − *College of Medicine and Health Sciences, Department of Biochemistry and Molecular Biology, United Arab Emirates University, AlAin 15551, United Arab Emirates*

Complete contact information is available at: https://pubs.acs.org/10.1021/acsomega.3c09732

Notes

The authors declare no competing financial interest.

■ ACKNOWLEDGMENTS

This project has been partially funded by *i)* Seed Grant (code: G00003544) from the College of Medicine and Health Sciences, United Arab Emirates University, *ii)* Start-Up Grant (code: G00003519), and *iii)* UAEU Strategic Research Program (via the Zayed Bin Sultan Al Nahyan Center for Health Sciences) grant (code: G00003650). We would like to thank OpenEye Scientific (https://www.eyesopen.com/) for providing us with the academic version of their software.

■ REFERENCES

(1) Patani, G. A.; LaVoie, E. J. Bioisosterism: Hspace0.167em A Rational Approach in Drug Design. *Chem. Rev.* **1996**, *96* (8), 3147−3176.
(2) Brown, N. *Bioisosteres in Medicinal Chemistry*; John Wiley & Sons, 2012.
(3) Langmuir, I. The Arrangement of Electrons in Atoms and Molecules. *J. Am. Chem. Soc.* **1919**, *41* (6), 868−934.
(4) Grimm, H. G. Structure and Size of the Non-metallic Hydrides Z. *Electrochem* **1925**, *31*, 474−480.
(5) Friedman, H. L. *Influence of isosteric replacements upon biological activity*; NAS-NRS Publication, 1951.
(6) Thornber, C. W. Isosterism and molecular modification in drug design. *Chem. Soc. Rev.* **1979**, *8* (4), 563.
(7) Burger, A. Isosterism and bioisosterism in drug design. *Prog. Drug Res.* **1991**, *37*, 287−371.
(8) Agalave, S. G.; Maujan, S. R.; Pore, V. S. Click Chemistry: 1,2,3-Triazoles as Pharmacophores. *Chem. - Asian J.* **2011**, *6* (10), 2696−2718.
(9) Ashok Philip, M. O. F. K. *Fundamentals of Medicinal Chemistry and Drug Metabolism*; Bentham Science Publishers, 2018.
(10) Batalha, P. N.; Forezi, L. S.M.; Lima, C. G.S.; Pauli, F. P.; Boechat, F. C.S.; de Souza, M. C. B.V.; Cunha, A. C.; Ferreira, V. F.; da Silva, F. d. C. Drug repurposing for the treatment of COVID-19: Pharmacological aspects and synthetic approaches. *Bioorganic Chemistry* **2021**, *106*, 104488.
(11) Meanwell, N. A. The Influence of Bioisosteres in Drug Design: Tactical Applications to Address Developability Problems. In *Topics in Medicinal Chemistry*; Springer: Berlin Heidelberg, 2013; pp. 283381.
(12) Bonandi, E.; Christodoulou, M. S.; Fumagalli, G.; Perdicchia, D.; Rastelli, G.; Passarella, D. The 1,2,3-triazole ring as a bioisostere in medicinal chemistry. *Drug Discovery Today* **2017**, *22* (10), 1572−1581.
(13) Brik, A.; Alexandratos, J.; Lin, Y.-C.; Elder, J. H.; Olson, A. J.; Wlodawer, A.; Goodsell, D. S.; Wong, C.-H. 1,2,3-Triazole as a Peptide Surrogate in the Rapid Synthesis of HIV-1 Protease Inhibitors. *ChemBiochem* **2005**, *6* (7), 1167−1169.
(14) Bourne, Y.; Kolb, H. C.; Radic, Z.; Sharpless, K. B.; Taylor, P.; Marchot, P. Freeze-frame inhibitor captures acetylcholinesterase in a unique conformation. *Proc. Natl. Acad. Sci. U. S. A.* **2004**, *101* (6), 1449−1454.
(15) Grob, N. M.; Schmid, S.; Schibli, R.; Behe, M.; Mindt, T. L. Design of Radiolabeled Analogs of Minigastrin by Multiple Amide-to-Triazole Substitutions. *J. Med. Chem.* **2020**, *63* (9), 4496−4505.
(16) Mohammed, I.; Kummetha, I. R.; Singh, G.; Sharova, N.; Lichinchi, G.; Dang, J.; Stevenson, M.; Rana, T. M. 1,2,3-Triazoles as Amide Bioisosteres: Discovery of a New Class of Potent HIV-1 Vif Antagonists. *J. Med. Chem.* **2016**, *59* (16), 7677−7682.
(17) Rahman, M. T.; Decker, A. M.; Laudermilk, L.; Maitra, R.; Ma, W.; Hamida, S. B.; Darcq, E.; Kieffer, B. L.; Jin, C. Evaluation of Amide Bioisosteres Leading to 1,2,3-Triazole Containing Compounds as GPR88 Agonists: Design, Synthesis, and Structure−Activity Relationship Studies. *J. Med. Chem.* **2021**, *64* (16), 12397−12413.
(18) Chrysina, E. D.; Bokor, É.; Alexacou, K.-M.; Charavgi, M.-D.; Oikonomakos, G. N.; Zographos, S. E.; Leonidas, D. D.; Oikonomakos, N. G.; Somsák, L. Amide-1,2,3-triazole bioisosterism: The glycogen phosphorylase case. *Tetrahedron: Asymmetry* **2009**, *20* (6−8), 733−740.
(19) Sahu, A.; Das, D.; Sahu, P.; Mishra, S.; Sakthivel, A.; Gajbhiye, A.; Agrawal, R. Bioisosteric Replacement of Amide Group with 1,2,3-Triazoles in Acetaminophen Addresses Reactive Oxygen Species-Mediated Hepatotoxic Insult in Wistar Albino Rats. *Chem. Res. Toxicol.* **2020**, *33* (2), 522−535.
(20) Kim, S.; Cho, M.; Lee, T.; Lee, S.; Min, H.-Y.; Lee, S. K. Design, synthesis, and preliminary biological evaluation of a novel triazole analogue of ceramide. *Bioorg. Mathsemicolon Med. Chem. Lett.* **2007**, *17* (16), 4584−4587.
(21) Malik, M. S.; Ahmed, S. A.; Althagafi, I. I.; Ansari, M. A.; Kamal, A. Application of triazoles as bioisosteres and linkers in the development of microtubule targeting agents. *RSC Med. Chem.* **2020**, *11* (3), 327−348.
(22) Christodoulou, M. S.; Mori, M.; Pantano, R.; Alfonsi, R.; Infante, P.; Botta, M.; Damia, G.; Ricci, F.; Sotiropoulou, P. A.; Liekens, S.; Botta, B.; Passarella, D. Click Reaction as a Tool to Combine Pharmacophores: The Case of Vismodegib. *ChemPluschem* **2015**, *80* (6), 938−943.
(23) Capdeville, R.; Buchdunger, E.; Zimmermann, J.; Matter, A. Glivec (STI571, imatinib), a rationally developed, targeted anticancer drug. *Nat. Rev. Drug Discov.* **2002**, *1* (7), 493−502.
(24) Buchdunger, E.; OtextquotesingleReilley, T.; Wood, J. Pharmacology of imatinib (STI571). *Eur. J. Cancer* **2002**, *38*, S28−S36.
(25) Iqbal, N.; Iqbal, N. Imatinib: A Breakthrough of Targeted Therapy in Cancer. *Chemother. Res. Pract.* **2014**, *2014*, 1−9.
(26) Cowan-Jacob, S. W.; Fendrich, G.; Floersheimer, A.; Furet, P.; Liebetanz, J.; Rummel, G.; Rheinberger, P.; Centeleghe, M.; Fabbro, D.; Manley, P. W. Structural biology contributions to the discovery of drugs to treat chronic myelogenous leukaemia. *Acta Crystallogr. D Biol. Crystallogr.* **2007**, *63* (1), 80−93.
(27) Arioli, F.; Borrelli, S.; Colombo, F.; Falchi, F.; Filippi, I.; Crespan, E.; Naldini, A.; Scalia, G.; Silvani, A.; Maga, G.; Carraro, F.; Botta, M.; Passarella, D. N-[2-Methyl-5-(triazol-1-yl)phenyl]-pyrimidin-2-amine as a Scaffold for the Synthesis of Inhibitors of Bcr-Abl. *ChemMedchem* **2011**, *6* (11), 2009−2018.
(28) Kumari, S.; Carmona, A. V.; Tiwari, A. K.; Trippier, P. C. Amide Bond Bioisosteres: Strategies, Synthesis, and Successes. *J. Med. Chem.* **2020**, *63* (21), 12290−12358.
(29) Arabi, A. A. Atomic and molecular properties of nonclassical bioisosteric replacements of the carboxylic acid group. *Future Med. Chem.* **2020**.
(30) Arabi, A. A. Routes to drug design via bioisosterism of carboxyl and sulfonamide groups. *Future Med. Chem.* **2017**, *9* (18), 2167−2180.
(31) Arabi, A. A.; Matta, C. F. Electrostatic potentials and average electron densities of bioisosteres in methylsquarate and acetic acid. *Future Med. Chem.* **2016**, *8* (4), 361−371.
(32) Matta, C. F.; Arabi, A. A.; Weaver, D. F. The bioisosteric similarity of the tetrazole and carboxylate anions: Clues from the topologies of the electrostatic potential and of the electron density. *Eur. J. Med. Chem.* **2010**, *45* (5), 1868−1872.
(33) Francisco, K. R.; Varricchio, C.; Paniak, T. J.; Kozlowski, M. C.; Brancale, A.; Ballatore, C. Structure property relationships of N-acylsulfonamides and related bioisosteres. *Eur. J. Med. Chem.* **2021**, *218*, 113399.
(34) Bolcato, G.; Heid, E.; Boström, J. On the Value of Using 3D Shape and Electrostatic Similarities in Deep Generative Methods. *J. Chem. Inf. Model* **2022**, *62* (6), 1388−1398.
(35) Mottishaw, J. D.; Erck, A. R.; Kramer, J. H.; Sun, H.; Koppang, M. Electrostatic Potential Maps and Natural Bond Orbital Analysis: Visualization and Conceptualization of Reactivity in Sanger's Reagent. *J. Chem. Educ.* **2015**, *92* (11), 1846−1852.

https://doi.org/10.1021/acsomega.3c09732
ACS Omega 2024, 9, 13172−13182

(36) Tasi, G.; Pálinkó, I. Using molecular electrostatic potential maps for similarity studies. In *Topics in Current Chemistry*; Springer: Berlin Heidelberg, 1995; pp. 4571.
(37) Osman, A. M. A.; Arabi, A. A. Quantum and Classical Evaluations of Carboxylic Acid Bioisosteres: From Capped Moieties to a Drug Molecule. *ACS Omega* **2022**, *8*, 588−598.
(38) Polêto, M. D.; Rusu, V. H.; Grisci, B. I.; Dorn, M.; Lins, R. D.; Verli, H. Aromatic Rings Commonly Used in Medicinal Chemistry: Force Fields Comparison and Interactions With Water Toward the Design of New Chemical Entities. *Front. Pharmacol.* **2018**, *9*, 395.
(39) Frisch, M. J.; Trucks, G. W.; Schlegel, H. B.; Scuseria, G. E.; Robb, M. A.; Cheeseman, J. R.; Scalmani, G.; Barone, V.; Mennucci, B.; Petersson, G. A.; Nakatsuji, H.; Caricato, M.; Li, X.; Hratchian, H. P.; Izmaylov, A. F.; Bloino, J.; Zheng, G.; Sonnenberg, J. L.; Hada, M.; Ehara, M.; Toyota, K.; Fukuda, R.; Hasegawa, J.; Ishida, M.; Nakajima, T.; Honda, Y.; Kitao, O.; Nakai, H.; Vreven, T.; Montgomery, J. A., Jr.; Peralta, J. E.; Ogliaro, F.; Bearpark, M.; Heyd, J. J.; Brothers, E.; Kudin, K. N.; Staroverov, V. N.; Kobayashi, R.; Normand, J.; Raghavachari, K.; Rendell, A.; Burant, J. C.; Iyengar, S. S.; Tomasi, J.; Cossi, M.; Rega, N.; Millam, J. M.; Klene, M.; Knox, J. E.; Cross, J. B.; Bakken, V.; Adamo, C.; Jaramillo, J.; Gomperts, R.; Stratmann, R. E.; Yazyev, O.; Austin, A. J.; Cammi, R.; Pomelli, C.; Ochterski, J. W.; Martin, R. L.; Morokuma, K.; Zakrzewski, V. G.; Voth, G. A.; Salvador, P.; Dannenberg, J. J.; Dapprich, S.; Daniels, A. D.; Farkas, O.; Foresman, J. B.; Ortiz, J. V.; Cioslowski, J.; Fox, D. J. *Gaussian 09*; Gaussian Inc: Pittsburgh PA, 2009.
(40) Keith, T. A. 2019 (aim.tkgristmill.com) TK Gristmill Software Overland Park KS USA. AIMAll (Version 19.10.12).
(41) Bader, R. F. *Atoms in Molecules: A Quantum Theory*; Oxford University Press: Oxford, UK, 1994.
(42) *The Quantum Theory of Atoms in Molecules: from Solid State to DNA and Drug Design*, Matta, C. F.; Boyd, R. J., Eds.; Wiley-VCH: Weinheim, Germany, 2007.
(43) Hawkins, P. C. D.; Geoffrey Skillman, A.; Warren, G. L.; Ellingson, B. A.; Stahl, M. T. Conformer Generation with OMEGA: Algorithm and Validation Using High Quality Structures from the Protein Databank and the Cambridge Structural Database. *J. Chem. Inf. Model* **2010**, *50*, 472−584.
(44) Mark, M. FRED and HYBRID docking performance on standardized datasets. *J. Comput.-Aided Mol. Des* **2012**, *26*, 897−906.
(45) McGann, M. FRED Pose Prediction and Virtual Screening Accuracy. *J. Chem. Inf. Model* **2011**, *51* (3), 578−596.
(46) Santa Fe, N. VIDA 4.4.0.4 OpenEye Scientific Software. http://www.eyesopen.
(47) Wood, D. J.; de Vlieg, J.; Wagener, M.; Ritschel, T. Pharmacophore Fingerprint-Based Approach to Binding Site Subpocket Similarity and Its Application to Bioisostere Replacement. *J. Chem. Inf. Model* **2012**, *52* (8), 2031−2043.
(48) Recnik, L.-M.; Kandioller, W.; Mindt, T. L. 1,4-Disubstituted 1,2,3-Triazoles as Amide Bond Surrogates for the Stabilisation of Linear Peptides with Biological Activity. *Molecules* **2020**, *25* (16), 3576.
(49) Proteau-Gagné, A.; Rochon, K.; Roy, M.; Albert, P.-J.; Guérin, B.; Gendron, L.; Dory, Y. L. Systematic replacement of amides by 1,4-disubstituted[1,2,3]triazoles in Leu-enkephalin and the impact on the delta opioid receptor activity. *Bioorg. Mathsemicolon Med. Chem. Lett.* **2013**, *23* (19), 5267−5269.
(50) Hur, S.; Bruice, T. C. The Mechanism of Cislessigreater-less/igreaterTrans Isomerization of Prolyl Peptides by Cyclophilin. *J. Am. Chem. Soc.* **2002**, *124* (25), 7303−7313.
(51) Tron, G. C.; Pirali, T.; Billington, R. A.; Canonico, P. L.; Sorba, G.; Genazzani, A. A. Click chemistry reactions in medicinal chemistry: Applications of the 1,3-dipolar cycloaddition between azides and alkynes. *Med. Res. Rev.* **2008**, *28* (2), 278−308.
(52) Hou, J.; Liu, X.; Shen, J.; Zhao, G.; Wang, P. G. The impact of click chemistry in medicinal chemistry. *Expert Opin. Drug Discovery* **2012**, *7* (6), 489−501.
(53) Cuozzo, A.; Daina, A.; Perez, M. A. S.; Michielin, O.; Zoete, V. SwissBioisostere 2021: Updated structural, bioactivity and physicochemical data delivered by a reshaped web interface. *Nucleic Acids Res.* **2022**, *50* (D1), D1382−D1390.

https://doi.org/10.1021/acsomega.3c09732
ACS Omega 2024, 9, 13172−13182